



The mechanical and morphological properties of 6 year-old cranial bone

Matthew T. Davis, Andre M. Loyd, Han-yu Henry Shen, Maura H. Mulroy, Roger W. Nightingale*, Barry S. Myers, Cameron Dale Bass

Department of Biomedical Engineering, Duke University, Box 90281, Durham, NC 27708-0281, United States

ARTICLE INFO

Article history:
Accepted 6 July 2012

Keywords:
Bone
Cranial bone
Pediatric
Biomechanics
Strength
Skull
Mechanical properties
Injury
Structure

ABSTRACT

Traumatic Brain Injury (TBI) is a leading cause of mortality and morbidity for children in the United States. The unavailability of pediatric cadavers makes it difficult to study and characterize the mechanical behavior of the pediatric skull. Computer based finite element modeling could provide valuable insights, but the utility of these models depends upon the accuracy of cranial material property inputs.

In this study, 47 samples from one six year-old human cranium were tested to failure via four point bending to study the effects of strain rate and the structure of skull bone on modulus of elasticity and failure properties for both cranial bone and suture. The results show that strain rate does not have a statistically meaningful effect on the mechanical properties of the six year-old skull over the range of strain rates studied (average low rate of 0.045 s^{-1} , average medium rate of 0.44 s^{-1} , and an average high rate of 2.2 s^{-1}), but that these properties do depend on the growth patterns and morphology of the skull. The thickness of the bone was found to vary with structure. The bending stiffness (per unit width) for tri-layer bone ($12.32 \pm 5.18 \text{ Nm}^2/\text{m}$) was significantly higher than that of cortical bone and sutures ($5.58 \pm 1.46 \text{ Nm}^2/\text{m}$ and $3.70 \pm 1.88 \text{ Nm}^2/\text{m}$ respectively). The modulus of elasticity was $9.87 \pm 1.24 \text{ GPa}$ for cranial cortical bone and $1.10 \pm 0.53 \text{ GPa}$ for sutures. The effective elastic modulus of tri-layer bone was $3.69 \pm 0.92 \text{ GPa}$. Accurate models of the pediatric skull should account for the differences amongst these three distinct tissues in the six year-old skull.

© 2012 Elsevier Ltd. All rights reserved.

1. Introduction

Traumatic brain injury (TBI) is the leading cause of death for the population under 24 years old, accounting for an estimated 30% of all accidental deaths (James, 1999; Schneier et al., 2006). Additionally, it is estimated that as many as 5.3 million people in the United States are currently living with a TBI-related long-term disability (Bushnik et al., 2003). Owing to the limited number of postmortem pediatric cadavers available (Prange et al., 2004), pediatric head biomechanics has not been investigated in congruity with its societal impact (Langlois et al., 2005).

Computational finite element models (FEMs) are commonly used in place of direct mechanical investigations of pediatric head injury (Coats, 2007; Coats et al., 2007; Klinich et al., 2002; Margulies and Thibault, 2000). FEMs have been used in the analysis of child safety restraints, seatbelts, and airbags. Accurate predictions, however, require accurate material properties. Among the most critical material properties needed are those of cranial bone, such as elastic modulus and ultimate stress and

strain. These properties drive the overall mechanical response of the head including skull fracture and brain response. Other methods, including inverse finite element optimization, couples experimentally observed force–deflection curves with computational models to reverse engineer the material properties of a given material (Guan et al., 2011).

The mechanical properties of adult bone have been obtained in the past using a variety of methods (Evans and Lissner, 1956; McElhaney et al., 1970; Roberts and Melvin, 1968; Wood, 1971). More recent efforts to publish data on pediatric specimens have focused on neonates and infants (Coats and Margulies, 2006; Margulies and Thibault, 2000; McPherson and Kriewall 1980a, 1980b). Margulies and Coats analyzed the properties' dependence on strain rate, region, and age for a collection of specimen ranging from 21 weeks gestation to 13 months old. Baumer et al. reported properties obtained via four-point-bending of infant porcine parietal bone to propose a correlation to human tissue (Baumer et al., 2009; Coats and Margulies, 2006). These studies found that the constitutive properties of pediatric cranial bone are age sensitive but not strain rate dependent for the rates tested. Prior research on the adult, however, has shown that these mechanical properties vary weakly with strain rate for bone (Carter and Hayes, 1976; McElhaney, 1966; Wood, 1971). Unfortunately,

* Corresponding author. Tel.: +1 919 660 5451; fax: +1 919 660 5362.
E-mail address: rwn@duke.edu (R.W. Nightingale)

no data has been published on rate dependency in calvaria in or near the six year-old cohort used in this study.

Extensive cranial growth occurs between the ages of 13 months and 18 years, however, the effect that this growth has on the mechanical properties of the pediatric skull during this transitional period remains largely undocumented. Although Kriewall and McPherson published data on the elastic modulus of a six year-old skull (7.1 GPa, mean thickness of 3.33 mm) they did not discuss the structure of the bones tested (Kriewall et al., 1980).

As periosteal tissues expand in response to the developing brain, the bones of the cranium move apart, straining the sutures and simultaneously creating space for and signaling for the growth of new bone. Thus, the primary direction of bone growth in the pediatric skull is toward the sutures (Cohen and Maclean, 2000; DuterLoo and Enlow, 2005). The bone also transitions from the single layered structure observed in early childhood to the tri-layer bone present in adults, which is comprised of a cortical table on both the ecto- and endo-cranial surface separated by a porous trabecular layer. This occurs by the simultaneous deposition of new bone on both the ectocranial and endocranial surfaces and resorption of the inner layer (Cohen and Maclean, 2000). These two modes of growth, resulting in the non-uniform development of the pediatric skull, may create regional variation in mechanical properties (Fig. 1).

The purpose of this paper is to study the mechanical properties of a six year-old skull to better understand how the child calvarium differs from that of both adults and neonates. One hypothesized difference is that modulus of elasticity and ultimate stress and strain of the cranial tissue will vary with region due to the growth pattern of the pediatric skull. Finally, it is also hypothesized that modulus and failure properties will not vary significantly with strain rate for the range of loading rates studied.

2. Methods

2.1. Specimen preparation

A single six year-old female cadaver (COD: germ cell malignancy, Weight: 60l bs, Height: 4'6" Ethnicity: Caucasian) was obtained in compliance with federal, state, local and institutional regulations. The calvarium was removed and 71 samples were cut from the frontal and parietal regions of the skull using a

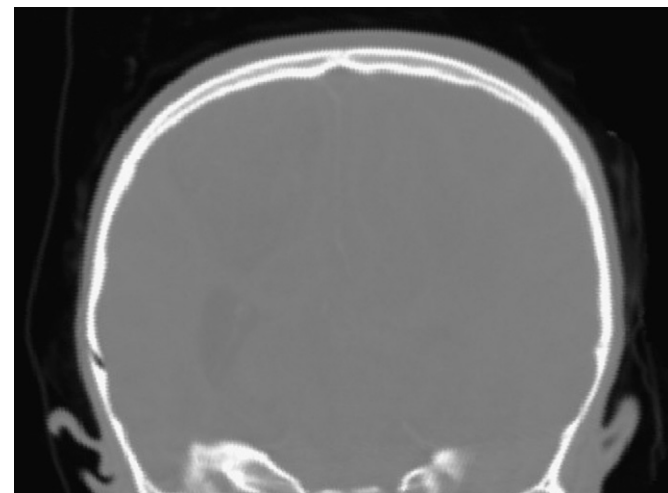


Fig. 1. An image of the cross-section of the intact skull showing the distribution of tri-layer and uni-layer bone. The oblique coronal view of the left and right parietal regions shown above indicates that the bone is thickest and most mature in the area surrounding the sagittal suture. The bone nearer the sides and the apexes are comprised of only cortical bone.

table mounted Dremel tool (Robert Bosch Tool Corporation, Mount Prospect, Illinois) with a 1/16" grinding bit. The suture samples were harvested perpendicular to and across the suture lines, and the bone samples were taken from the parietal and frontal regions of the calvaria. The samples were cut so that their dimensions were 30–35 mm in length and 3–5 mm in width. The bone was moistened with a saline drip during the process. Each sample was then fixed into ABS plastic containers of rectangular geometry using polymethylmethacrylate (PMMA), leaving approximately 12 mm of bone exposed. Each of the bone samples was then wrapped in gauze soaked in saline (0.9% NaCl) to keep the bones moist throughout the testing process and stored separately in a refrigerator at 5 °C for 1–3 days while testing was carried out. During this time each sample was scanned using micro-CT at 50 μ resolution.

2.2. Testing procedure

Bending tests were performed using a custom-built four-point-bending apparatus attached to a Bose ElectroForce 3200[®] linear actuator (Bose, Framingham, Massachusetts). The rig was designed to minimize friction by the use of steel roller pins mounted in ABEC-7 ball bearings as supports. Displacement control failure tests were run at three different displacement rates (4 mm/s, 40 mm/s, 400 mm/s). Because the relationship between displacement of the beam supports and the angle of beam deflection is non-linear, the corresponding average strain rates were approximately 0.045 s⁻¹, 0.44 s⁻¹, and 2.2 s⁻¹, with some variation due to the variation in specimen size. The force during testing was recorded using a Honeywell Model-31 222.5 N load cell (Morristown, New Jersey). End brackets were lubricated with light machine oil and placed onto the stainless steel roller supports of the four-point-bending apparatus. High speed digital imaging data from a Phantom video camera (Vision Research, Inc., Wayne, NJ) was recorded for each failure test (2000 frames per second for low rate, 7700 frames per second for medium and high rate) and later used to determine the angle of displacement undergone by each specimen using TEMA tracking software (Photo-Sonics, Inc., Burbank, CA).

2.3. Analysis

The geometry of the specimen was determined using the micro-CT scans taken before testing and photographs taken after failure. To avoid the uncertainties of stress-concentrations and other end-effects, we did not analyze any samples that broke in or near the PMMA-bone interface. The cross-sectional dimension of each bone was obtained by measurement of the smallest cross-sectional area of each specimen.

Stress was estimated by assuming that the samples behave like solid beams of constant cross-section as:

$$\sigma = \frac{My}{I} \quad (1)$$

where M is the bending moment, y is the half-thickness of the sample at the location of failure, and I is the moment of inertia of the rectangular cross section ($I = bh^3/12$).

Using the same assumptions, an estimate of the tensile strain on the outer surface of the bone was obtained by considering the radius of curvature of the sample in bending and from tracking the angle of rotation of the end pieces by the equation:

$$\varepsilon = \frac{2y\Phi}{L} \quad (2)$$

where y is the same half-thickness measurement as the stress equation above, L is the original length of the beam exposed, and Φ is the angle of rotation of the end pieces (Fig. 2). The modulus of elasticity was obtained by a constrained minimization of the residuals of a Ramberg–Osgood piecewise linear and power law curve fit to the stress–strain data using a 0.2% offset as the cutoff for linearity. For the case of the sandwich structure specimens and the suture specimens we use the simplifying assumption that the bone has a homogeneous cross section to simplify the analysis and because we are interested in the bulk load response of the specimens. For this reason, the modulus of elasticity of these samples should be considered to be an *effective* modulus of a composite structure model of the tissue, and does not reflect the true modulus of any one constituent material of the bone.

The bending stiffness is the product of this modulus of elasticity and the area moment inertia (EI) and used as a metric of bending stiffness. This was calculated for each specimen base on the effective elastic modulus and the microCT cross-section. Because the width of each specimen varied as a result of the harvesting procedure, the bending stiffnesses were normalized by the width and are thus reported in units of Nm²/m.

The categorization of samples based on structure was performed using the micro-CT scans and Avizo imaging software (VSG, Burlington, MA). The cross-sectional profiles of the beam were captured at the location of failure and the mean grayscale value in each pixel row within the bone was plotted against thickness. A local minimum in these plots indicated the presence of a porous layer or the beginnings of a resorptive process, and thus indicated that the bone was not

Download English Version:

<https://daneshyari.com/en/article/872232>

Download Persian Version:

<https://daneshyari.com/article/872232>

[Daneshyari.com](https://daneshyari.com)